Numerical Solutions of the Schrödinger Equation

Anders W. Sandvik, Department of Physics, Boston University

1 Introduction

The most basic problem in quantum mechanics is to solve the stationary Schrödinger equation,

$$-\frac{\hbar^2}{2m}\nabla^2\Psi_n(\vec{x}) + V(\vec{x})\Psi_n(\vec{x}) = E_n\Psi_n(\vec{x}), \tag{1}$$

for the energy eigenvalues E_n and the associated energy eigenfunctions (stationary states) Ψ_n. There are a number of important cases for which the stationary Schrödinger equation can be solved analytically, e.g., the harmonic oscillator (in any number of dimensions) and the hydrogen atom. However, in most cases of practical interest (in, e.g., atomic, molecular, and solid-state physics) exact or approximate numerical methods must be employed.

Here we will first discuss solutions of the Schrödinger equation (1) in one dimension, which is a problem almost identical to solving the radial wave function for spherically symmetric potentials in two or three dimensions. We will derive and use Numerov's method, which is a very elegant fifth-order scheme (i.e., with single-step error scaling as the sixth power of the space step Δ_x) for equations of the Schrödinger form.

In dimensions higher than one, if the potential cannot be separated, i.e., it cannot be written as a product of potentials of the different coordinates, solving the Schrödinger equation numerically is in general quite a complex problem. This stems from the large number of points needed on a grid and the requirement to satisfy boundary conditions on a whole curve or surface, instead of just at two points in one dimension. In practice, variational methods are therefore often used, where the wave function is expanded in an incomplete set of conveniently chosen basis states (i.e., one not spanning the full Hilbert space and hence leading to energies higher than the true eigenvalues E_n). This reduces the calculation to an eigenvalue problem (or generalized eigenvalue problem in the case of a non-orthogonal basis) in a discrete finite-dimensional space. We will show some examples of variational calculations and discuss the matrix diagonalizations that have to be performed to solve the resulting eigenvalue problems. We will also discuss a grid method, based on a set of basis functions describing particles localized inside a small finite volume, in which case a sparse-matrix diagonalization technique—the Lanczos method—can be used to obtain the low-lying states.

In addition to stationary solutions of the Schrödinger equation, we will discuss the time dependence of wave functions. The time-dependence of a stationary state only involves a phase factor;

$$\Psi_n(t) = e^{-itE_n/\hbar}\Psi_n(0), \tag{2}$$

where $\Psi_n(0) = \Psi_n$. Thus, if an arbitrary state Ψ at $t = 0$ is expanded in the stationary states,

$$\Psi = \sum_n C_n\Psi_n, \quad C_n = \int dx^d\Psi_n(\vec{x})\Psi(\vec{x}), \tag{3}$$

where d is the number of dimensions, its time dependence is given by

$$\Psi(t) = \sum_n C_n \mathrm{e}^{-itE_n/\hbar} \Psi_n. \tag{4}$$

However, it is not always practical to solve for all the energy eigenstates, and one can alternatively directly solve the time dependent Schrödinger equation,

$$i\hbar \frac{\partial \Psi(\vec{x})}{\partial t} = H\Psi(\vec{x}, t), \tag{5}$$

where the Hamiltonian is

$$H = -\frac{\hbar^2}{2m}\nabla^2 + V(\vec{x}). \tag{6}$$

The time dependent equation has the formal solution

$$\Psi(t) = \mathrm{e}^{-itH/\hbar}\Psi(0), \tag{7}$$

which can be easier to work with than the underlying partial differential equation (5). Here we will briefly discuss numerical solutions of the time dependent Schrödinger equation using the formal solution (7) with the time evolution operator for a short time Δ_t approximated using the so-called Trotter decomposition;

$$\mathrm{e}^{-\Delta_t H/\hbar} = \mathrm{e}^{-\delta_t \hbar \nabla^2/2m}\mathrm{e}^{-\Delta_t V(\vec{x})/\hbar} + O(\Delta_t)^2, \tag{8}$$

and higher-order versions of it. By alternating between the wave function $\Psi(\vec{x})$ in the position basis and its Fourier transform $\Psi(\vec{k})$, the time evolution can be carried out by simple multiplications. We will discuss the Fast-Fourier-Transform method, which should be used to efficiently carry out the long series of Fourier and inverse Fourier transformations needed to propagate the wave function this way for a large number of time steps.

2 One-dimensional stationary Schrödinger equations

In one dimension, the time independent Schrödinger equation (1) reduces to

$$-\frac{\hbar^2}{2m}\frac{d^2\Psi(x)}{dx^2} + V(x)\Psi(x) = E\Psi(x). \tag{9}$$

For a spherically symmetric potential in three dimensions, the Schrödinger equation factorizes into a radial and angular part,

$$\Psi_{L,L_z,n}(\vec{x}) = R_{L,n}(r)Y_{L,L_z}(\phi, \Theta), \tag{10}$$

where $Y_{L,L_z}(\phi, \Theta)$ are the spherical harmonics and the radial function satisfies the equation

$$\left(-\frac{\hbar^2}{2m}\frac{1}{r}\frac{d^2}{dr^2}r + \frac{L(L+1)\hbar^2}{2mr^2} + V(r) \right) R_{L,n}(r) = E_{L,n}R_{L,n}(r). \tag{11}$$

For a two-body system with a central potential, the mass m should be replaced by the reduced mass, but otherwise the equations are the same. Defining the function

$$U_{L,n}(r) = rR_{L,n}(r), \tag{12}$$

a simpler radial equation is obtained;

$$\left(-\frac{\hbar^2}{2m}\frac{d^2}{dr^2} + \frac{L(L+1)h^2}{2mr^2} + V(r)\right)U_{L,n}(r) = E_{L,n}U_{L,n}(r).\tag{13}$$

This is of the same form as the one-dimensional Schrödinger equation (9), apart from the fact that $-\infty < x < \infty$ but $r \geq 0$, and the presence of the repulsive "centrifugal barrier" which effectively contributes to the potential energy.

2.1 Numerov's algorithm

The one-dimensional Schrödinger equation (9) and the reduced radial equation (13) can both be written in the form

$$\Psi''(x) = f(x)\Psi(x).\tag{14}$$

To solve this type of equation numerically, we discretize the coordinate x using a uniform grid; $x_k = k\Delta_x$. We could now in principle proceed to rewrite the second-order differential equation as two coupled first-order equations, as we did in the case of the classical equations of motion, and then use, e.g., the Runge-Kutta method to integrate these. However, for the particular type of second order equation (14), a much simpler and very elegant scheme can be constructed which is of one higher order, i.e., with step error $O(\Delta_x^6)$. It is known as Numerov's method, and is derived by adding the Taylor expansion for $\Psi(x_{k+1}) = \Psi(x_k + \Delta_x)$,

$$\Psi(x_{k+1}) = \Psi(x_k) + \sum_{n=1}^{\infty}\frac{(-1)^n}{n!}\Delta_x^n\Psi^{(n)}(x_k),\tag{15}$$

and the corresponding expansion for $\Psi(x_{k-1})$, resulting in

$$\Psi(x_{k+1}) + \Psi(x_{k-1}) = 2\Psi(x_k) + \Delta_x^2\Psi''(x_k) + \frac{1}{12}\Delta_x^4\Psi^{(4)}(x_k) + O(\Delta_x^6).\tag{16}$$

Defining the central difference operator, acting on an arbitrary function $g(x)$,

$$\begin{aligned}\delta g(x) &= g(x + \Delta_x/2) - g(x - \Delta_x/2)\\ \delta^2 g(x) &= \delta[\delta g(x)] = g(x + \Delta_x) - 2g(x) + g(x - \Delta_x),\end{aligned}\tag{17}$$

Eq. (16) can be written as

$$\delta^2\Psi(x_k) = \Delta_x^2\Psi''(x_k) + \frac{1}{12}\Delta_x^4\Psi^{(4)}(x_k) + O(\Delta_x^6).\tag{18}$$

Here we do not know the fourth derivative, but we can write it as a central difference of the second derivative, using the above equation itself with the fourth-order term neglected:

$$\Delta_x^2\Psi^{(4)}(x_k) = \Delta_x^2[\Psi''(x_k)]'' = \delta^2\Psi''(x_k) + O(\Delta_x^4).\tag{19}$$

Hence, Eq. (18) can be written as

$$\delta^2\Psi(x_k) = \Delta_x^2\Psi''(x_k) + \frac{1}{12}\Delta_x^2\delta^2\Psi''(x_k) + O(\Delta_x^6).\tag{20}$$

This is a general result. Now, for the equation type (14) that we are intrested in, we can replace $\Psi''(x_k)$ by $f(x_k)\Psi(x_k)$ and obtain

$$\delta^2\Psi(x_k) = \Delta_x^2 f(x_k)\Psi(x_k) + \frac{1}{12}\Delta_x^2\delta^2[f(x_k)\Psi(x_k)] + O(\Delta_x^6), \tag{21}$$

or, with the abbreviated notation $g_n = g(x_n)$,

$$\Psi_{k+1} - 2\Psi_k + \Psi_{k-1} = \Delta_x^2 f_k\Psi_k + \frac{1}{12}\Delta_x^2[f_{k+1}\Psi_{k+1} - 2f_k\Psi_k + f_{k-1}\Psi_{k-1}] + O(\Delta_x^6), \tag{22}$$

where there should be no confusion with the nth eigenfunction, denoted $\Psi_n(x)$. Introducing a new function,

$$\phi_k = \Psi_k(1 - \Delta_x^2 f_k/12), \tag{23}$$

a simpler form corresponding to (22) is obtained;

$$\phi_{k+1} = 2\phi_k - \phi_{k-1} + \Delta_x^2 f_k\Psi_k + O(\Delta_x^6). \tag{24}$$

Comparing this with the rather complex fourth-order Runge-Kutta formula, this is clearly a very elegant fifth-order scheme.

2.2 Boundary conditions and energy finding strategy

In general the eigenfunctions $\Psi_n(x)$ and $U_{L,n}(r)$ are defined for all $-\infty < x < \infty$ and $r \geq 0$, respectively. Numerically we have to restrict the integration to within a finite range, however. Appropriate boundary conditions have to be imposed at the two end points. In the case of the reduced radial wave function, normalizability requires $U_{L,n}(0) = 0$ because the full radial wave function is obtained by multiplying it with $1/r$, according to (12). For $r \to \infty$ one can often obtain an asymptotic form, and this can be used to construct starting values $U_{L,n}(r_{max})$ and $U_{L,n}(r_{max} - \Delta_r)$ for integrating toward the center (one should then check the convergence of the result as r_{max} is increased). Asymptotic forms $\Psi_n(x \to \pm\infty)$ can similarily be found for one-dimensional problems, and they can be used for boundary conditions at $x = \pm x_{max}$, or there may be "hard walls" beyond which the potential is considered infinite and the wave function vanishes. Note that the starting values do not have to correspond to a normalized wave function; normalization can be carried out after the integration. As an example, with a hard wall at $x = x_0$ one can thus start with $\Psi(x_0) = 0$ and $\Psi(x_0 + \Delta_x) = 1$.

For the Schrödinger equation (9), setting $\hbar = m = 1$, we have $f(x) = 2[V(x) - E]$. If we have used boundary conditions to generate Ψ_0 and Ψ_1 (at one end of the integration range starting at x_0) and then calculate ϕ_0 and ϕ_n according to Eq. (23), a Fortran code segment for integrating a total of `nx` steps (to the other end of the integration range) can look like this:

```
do ix=2,nx
  q2=dx2*f1*psi(ix-1)+2.d0*q1-q0
  q0=q1; q1=q2
  f1=2.d0*(potential(x0+dx*dble(ix))-energy)
  psi(ix)=q1/(1.d0-dx2*f1)
end do
```
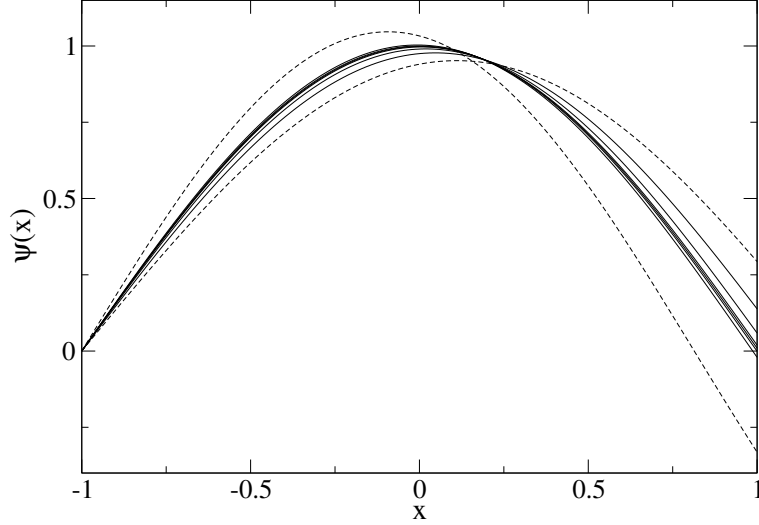
Figure 1: Wave functions generated in the shooting method for a potential well with infinitely repulsive walls. The dashed curves show the wave functions obtained with the bracketing energies $E^1 = 1.0$ and $E^2 = 1.5$. The other curves were obtained using bisection to gradually approach the boundary condition $\Psi(1) = 0$. With the two bracketing energies used, the ground state, for which the exact wave function $\Psi(x) = \cos(\pi x/2)$, is obtained.

where `dx2`=Δ_x^2, variables `q0,q1,q2` have been used for $\phi_{k-1}, \phi_k, \phi_{k+1}$, and `psi(k)` is the actual wave function $\Psi(x_k)$. The potential energy is here given by a function `potential(x)`, and the energy, which typically will be a current guess for the actual energy sought, is stored in `energy`. If the resulting `psi(nx)` satisfies the appropriate boundary condition a solution has been found; if not the energy has to be adjusted and another run through the loop has to be perfomed.

An efficient way to systematically adjust the energy toward a solution is to use bisection (recall Homework assignment 1). Denote by $\delta(E)$ the deviation of the wave function Ψ_{N_x} (now assumed normalized) at the end of the integration range from the boundary condition $\Psi_{N_x} = \Psi_{N_x}^b$ to be satisfied there when the energy used in the integration is E. We first search for two energies E^1 and E^2 leading to different signs of δ, i.e, $\delta(E^1)\delta(E^2) \leq 0$. These energies must bracket an eigenvalue E_n (or an odd number oif eigenvalues). Such a bracketing pair can simply be searched for by carrying out the integration using energies $E = E^0 + k\Delta_E$, $k = 0, 1, \ldots$, until the sign of δ changes (assuming that there is an eigenvalue with energy $> E_0$, and that the increment Δ_E is small enough for there not to be two eigenvalues within one step). When such a pair E^1, E^2 and has been found, an integration is carried out using $E = (E^1 + E^2)/2$, and depending on whether $\delta(E^3)\delta(E^1)$ is positive or negative the pair E^1, E^3 or E^2, E^3 is used as the bracketing pair in a repetition of the above procedure. This bisection is continued until either the difference between the bracketing energies or the deviation $|\delta|$ is smaller than some ϵ corresponding to a sufficiently accurate solution. This technique for gradually refining the solution is often called the "shooting method".

Fig. 1 illustrates the shooting method applied to the square well potential with infinite repulsion for $|x| > 1$ and $V(x) = 0$ for $|x| \leq 1$. The integration was started at $x = -1$, with the boundary condition $\Psi(-1) = 0$ and $\Psi(-1+\Delta_x) = 1$, with the step size $\Delta_x = 0.002$. The wave functions were
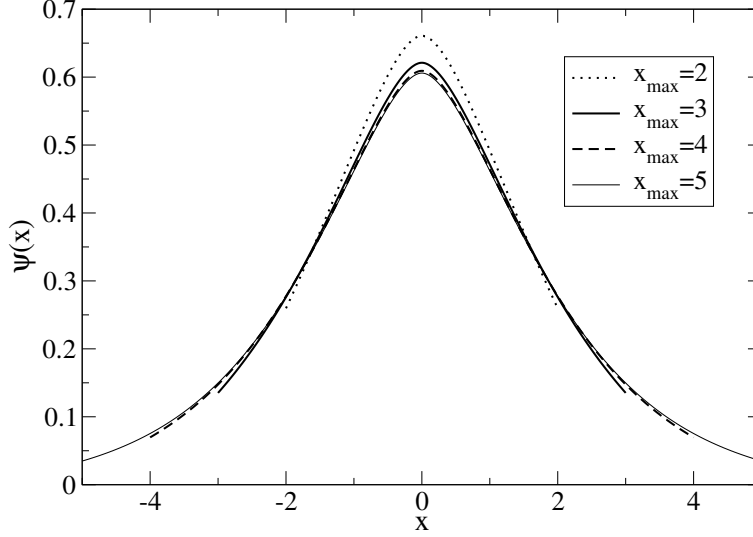
Figure 2: Wave function for the potential $V(x) = -\exp\left(-\sqrt{|x|}\right)$ integrated between $-x_{\max}$ and $x_{\max}$ with $x_{\max} = 2, 3, 4, 5$, using the asymptotic form $\Psi(x \to \pm\infty) \sim \exp\left[-|x|\sqrt{2(V(\pm\infty) - E)}\right]$ applied at $x = -x_{\max}$ and $x = -x_{\max} + \Delta_x$, and requiring $\Psi(x_{\max}) = \Psi(-x_{\max})$.

normalized after each integration, and the deviation of the boundary value $\Psi(1)$ from 0 was used for bisection. Using initial energies E^1, E^2 bracketing the exact ground state energy $E_0 = \pi^2/8$ of this system, the energy after a large number of bisections converged to $E = 1.233700550136$, which agrees with the true ground state energy to 9 decimal places.

For "soft" potentials, asymptotic forms for $x \to \pm\infty$ can typically be derived, which can then be applied at the ends of a finite integration range $[-x_{\max}, x_{\max}]$ if $x_{\max}$ is large. If the potential approaches a constant at long distances the asymptotic solution for a bound state is $\Psi(x \to \pm\infty) \sim \exp\left[-|x|\sqrt{2(V(\pm\infty) - E)}\right]$. Depending on exactly how the constant potential is approached, there can be corrections to this form, which typically can be neglected as long as $x_{\max}$ is sufficiently large. The asymptotic form can be applied at $x = -x_{\max}$ and $x = -x_{\max} + \Delta_x$ to start the integration, and at the other end point one can use $\Psi(x_{\max}) = -\Psi(x_{\max})$ (strictly only under the assumption that the potential has the same long-distance form form $x \to \pm\infty$, but if $x_{\max}$ is sufficiently large for the wave function to be very small at both boundaries this condition should always work well). In order to make sure that $x_{\max}$ is chosen sufficiently large, one should compare solutions obtained with different choises. An illustration of the dependence of the solution on $x_{\max}$ is shown in Fig. 2 for an exponentially decaying attractive potential. Here the wave functions have been normalized using only the integral of the Ψ^2 in the range $[-x_{\max}, x_{\max}]$, and hence the magnitude of the resulting wave function within this range larger than the true wave function.

It should be pointed out that even if the boundary condition used at long distances is not completely correct, the induced errors will typically only affect the wave function close to $\pm x_{\max}$, as long as $x_{\max}$ is sufficiently large. Fig. 3 shows an example of this, for the same potential as the one considered in Fig. 2.

The program with which the above examples were studied is available on the course web site in the file 'schrod1d.f90'.
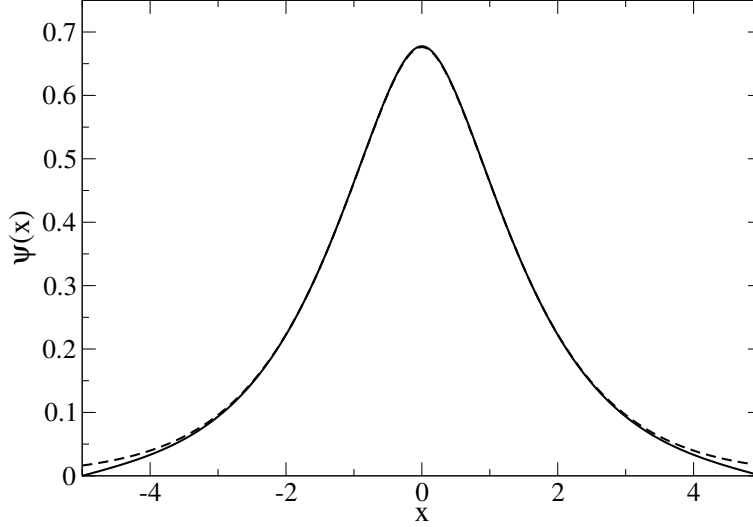
Figure 3: Wave function for the potential $V(x) = -e^{-|x|}$ integrated between $x = -5$ and 5, with the asymptotically correct boundary condition $\Psi(x) \sim \exp\left[-|x|\sqrt{2(V(\pm\infty) - E)}\right]$ (dashed curve) applied at $-x_{\max}$ and $-x_{\max} + \Delta_x$, and an incorrect boundary condition $\Psi(-x_{\max}) = 0$, $\Psi(-x_{\max} + \Delta_x) = 1$ (solid curve).

3 Variational methods

In order to numerically solve a two- or three-dimensional Schrödinger equation for a non-separable potential, one can in principle use some generally applicable grid-based technique for boundary-value partial differential equations, such as the finite-element method. However, the large number of grid points needed often makes such approaches too time-consuming in practice (but they are used in some applications). Approximate but systematically controllable *variational methods* are therefore predominant in large-scale calculations in atomic, molecular, and solid-state physics.

In general a variational calculation amounts to assuming a form $\Psi_{\{p_i\}}(\vec{x})$ of the wave function, with a number of adjustable parameters p_i, and finding the parameters that minimize the energy expectation value (the energy functional)

$$E[\Psi_{\{p_i\}}] = \frac{\langle \Psi_{\{p_i\}} | H | \Psi_{\{p_i\}} \rangle}{\langle \Psi_{\{p_i\}} | \Psi_{\{p_i\}} \rangle}. \tag{25}$$

The minimation is achieved by finding parameters such that the variation of the the energy functional, i.e., the first-order change in the energy due to infinitesimal changes in any of the parameters p_i, vanishes, i.e., $dE[\Psi_{\{p_i\}}]/dp_i = 0$ for all p_i. Since the states $\Psi_{\{p_i\}}$ span only a subspace of the full Hilbert space, energies calculated this way are always higher than the true eigenvalues.

In general, if the wave function $\Psi_{\{p_i\}}$ is a nonlinear function of the parameters, the variational calculation amounts to a very complex optimization problem. On the other hand, if $\Psi_{\{p_i\}}$ is linear in all the parameters, i.e., it is a linear combination of conveniently chosen basis states (which can

be specifically adapted to the potential under study),

$$\Psi_{\{p_i\}}(\vec{x}) = \sum_{i=1}^{N} p_i \phi_i(\vec{x}), \tag{26}$$

the minimization procedure is straight-forward, amounting to solving the Schrödinger equation in matrix form in a subspace of the full Hilbert space. As the size of the basis is increased, or the basis states are improved, the true energies are approached from above. Here we will discuss and show examples of variational calculations with orthogonal as well as non-orthogonal basis vectors. We will first discuss the general form of the Schrödinger equation written as a matrix diagonalization problem.

3.1 The Schrödinger equation in matrix form

The Schrödinger equation (1) for the stationary wave functions can be cast in a matrix form if a discrete basis is used instead of the continuous real-space position basis spanned by the states $|\vec{x}\rangle$. To see this, we begin by recalling some quantum mechanics formalism.

A state $|\Psi\rangle$ is related to its real-space wave function $\Psi(\vec{x})$ through

$$|\Psi\rangle = \int dx^d \Psi(\vec{x}) |\vec{x}\rangle, \tag{27}$$

where $|\vec{x}\rangle$ is a basis vector in the position basis (i.e., describing a particle localized at the point $\vec{x}$). Using the fact that $\langle \vec{x}|\vec{y}\rangle = \delta(\vec{x} - \vec{y})$, the wave function is formally obtained from the overlap with the position states;

$$\langle \vec{x}|\Psi\rangle = \int dy^d \Psi(\vec{y}) \langle \vec{x}|\vec{y}\rangle = \int dy^d \Psi(\vec{y}) \delta(\vec{x} - \vec{y}) = \Psi(\vec{x}). \tag{28}$$

For a complete discrete set of orthonormal basis states $\{|k\rangle\}$, any state $|\Psi\rangle$ can be expanded as

$$|\Psi\rangle = \sum_k C_k |k\rangle, \tag{29}$$

where normalization of $|\Psi\rangle$ implies that

$$\sum_k |C_k|^2 = 1. \tag{30}$$

The real-space wave function corresponding to the state $|k\rangle$ is denoted $\phi_k(\vec{x})$, i.e.,

$$|k\rangle = \int dx^d \phi_k(\vec{x}) |\vec{x}\rangle. \tag{31}$$

Because of orthonormality $\langle p|k\rangle = \delta_{pk}$, and hence in Eq. (29) the individual expansion coefficients $C_k = \langle k|\Psi\rangle$. In terms of the wave functions, the overlaps (scalar products) are given by

$$\langle k|\Psi\rangle = \int dx^d \int dy^d \phi_k^*(\vec{x}) \Psi(\vec{y}) \langle \vec{x}|\vec{y}\rangle = \int dx^d \phi_k^*(\vec{x}) \Psi(\vec{x}). \tag{32}$$

8

The most familiar example of a discrete basis is the the momentum basis defined in a finite box with periodic boundary conditions. In that case the basis functions are

$$\phi_{\vec{k}}(\vec{x}) = \frac{1}{\sqrt{V}}\exp(-i\vec{k}\cdot\vec{x}). \tag{33}$$

and the expansion coefficients $C_{\vec{k}}$ are thus given by the Fourier transform of the wave function

$$C_{\vec{k}} = \frac{1}{\sqrt{V}}\int dx^d e^{-i\vec{k}\cdot\vec{x}}\Psi(\vec{x}), \tag{34}$$

where $V = L^d$ is the volume of the box. The allowed wave vectors satisfying the periodic boundary conditions are, in three dimensions,

$$\vec{k} = (k_x, k_y, k_z) = \left(n_x\frac{2\pi}{L}, n_y\frac{2\pi}{L}, n_z\frac{2\pi}{L}\right), \tag{35}$$

where n_x, n_y, n_z are integers.

To construct the Schrödinger equation

$$H|\Psi\rangle = E|\Psi\rangle, \tag{36}$$

in any orthonormal basis $\{|k\rangle\}$ we simply use the expansion (29), giving

$$\sum_k C_k H|k\rangle = E\sum_k C_k|k\rangle, \tag{37}$$

where the problem now is to find sets of coefficients C_k (the wave function in the k basis) that satisfy the equation along with corresponding eigen energies. We can write

$$H|k\rangle = \sum_p H_{pk}|p\rangle, \quad H_{pk} = \langle p|H|k\rangle, \tag{38}$$

and hence

$$\sum_p \sum_k C_k H_{pk}|p\rangle = E\sum_k C_k|k\rangle. \tag{39}$$

Since the basis vectors are orthogonal, the terms corresponding to each state have to be satisfied individually, i.e.,

$$\sum_k C_k H_{pk} = EC_p, \tag{40}$$

for all p. All these equations can be written collectively as a matrix equation;

$$\begin{pmatrix} H_{11} & H_{12} & \cdots \\ H_{21} & H_{22} & \\ \vdots & & \ddots \end{pmatrix}\begin{pmatrix} C_1 \\ C_2 \\ \vdots \end{pmatrix} = E\begin{pmatrix} C_1 \\ C_2 \\ \vdots \end{pmatrix} \tag{41}$$

This is the Schrödinger equation in the k-basis, written more compactly as

$$\mathbf{HC} = E\mathbf{C}. \tag{42}$$

Solving it corresponds to diagonalizing the Hamiltonian matrix $\mathbf{H}$.

3.2 Variational calculation with orthogonal basis states

We now consider a truncated orthonormal basis, and so the wave function resulting from a linear variational calculation in this basis belongs to the subset of wave functions that can be written as linear combinations of a finite number N of orhogonal normalized basis states $|k\rangle$;

$$|\Psi\rangle = \sum_{k=1}^{N} C_k |k\rangle, \quad \langle k|p\rangle = \delta_{kp}. \tag{43}$$

It appears intuitively clear that the variational energy eigenstates in this case should be simply obtained by solving the matrix Schrrödinger equation (41) in the N-dimensional Hilbert space, i.e,

$$\begin{pmatrix} H_{11} & H_{12} & \cdots & H_{1N} \\ H_{21} & H_{22} & \cdots & H_{2N} \\ \vdots & & \ddots & \vdots \\ H_{N1} & H_{N2} & \cdots & H_{NN} \end{pmatrix} \begin{pmatrix} C_1 \\ C_2 \\ \vdots \\ C_N \end{pmatrix} = E \begin{pmatrix} C_1 \\ C_2 \\ \vdots \\ C_N \end{pmatrix}. \tag{44}$$

This is indeed the case, but since we will later consider non-orthonormal basis states, for which the variational calculation is slightly different, we will discuss the formal proof, which can be modified to find the correct way to proceed also for non-orthonormal states. The energy can be written as

$$E = \frac{\langle \Psi|H|\Psi\rangle}{\langle \Psi|\Psi\rangle} = \frac{\sum_{kp} C_k C_p^* H_{kp}}{\sum_k C_k^* C_k}. \tag{45}$$

We want to find expansion coefficients such that the leading-order variation of the energy under small changes in the expansion coefficients vanishes. Consider a change δ_q in one of the coefficients C_q, which also implies a change δ_q^* in its complex conjugate. Neglecting the terms quadratic in δ_q, the energy is

$$E(\delta_q) = \frac{\sum_{kp} C_k C_p^* H_{pk} + \sum_k (C_k \delta_q^* H_{qk} + \delta_q C_k^* H_{kq})}{\sum_k C_k C_k^* + C_q \delta_q^* + \delta_q C_q^*}, \tag{46}$$

which to leading order can be written as

$$E(\delta_q) = \left(E + \frac{\sum_k (C_k \delta_q^* H_{qk} + \delta_q C_k^* H_{kq})}{\sum_k C_k C_k^*} \right) \left(1 - \frac{C_q \delta_q^* + \delta_q C_q^*}{\sum_k C_k C_k^*} \right). \tag{47}$$

The leading-order energy shift is hence

$$E(\delta_q) - E = \frac{\sum_k (C_k \delta_q^* H_{qk} + \delta_q C_k^* H_{kq})}{\sum_k C_k C_k^*} - E \frac{C_q \delta_q^* + \delta_q C_q^*}{\sum_k C_k C_k^*}, \tag{48}$$

and for this to vanish we must have

$$\sum_k (\delta_q^* C_k H_{qk} + \delta_q C_k^* H_{kq}) = E(C_q \delta_q^* + \delta_q C_q^*). \tag{49}$$

Since $H_{kq} = H_{qk}^*$ this condition can be reduced exactly to Eq. (40), and we have thus shown that the condition for energy minimization is that the matrix Schrödinger equation (44) is satisfied.

3.3 Matrix diagonalization

In principle, the eigenvalues λ_n, $n = 1, \ldots, N$, of an $N \times N$ matrix $\mathbf{A}$ can be obtained by solving the secular equation,

$$\det[\mathbf{A} - \lambda \mathbf{I}] = 0, \tag{50}$$

where $\mathbf{I}$ is the unit matrix. The eigenvector $\mathbf{v}_n$ corresponding to an eigenvalue λ_n can subsequently be obtained by solving the matrix equation (set of linear coupled equations)

$$\mathbf{A}\mathbf{v}_n = \lambda_n \mathbf{v}_n. \tag{51}$$

However, since the secular equation is very complex for a large matrix, this method is not used in practice. Most matrix diagonalization methods are based on an iterative search for a unitary transformation $\mathbf{D}$ for which

$$\mathbf{D}^{-1}\mathbf{A}\mathbf{D} = \mathbf{E}, \tag{52}$$

where $\mathbf{E}$ is the diagonal eigenvalue matrix and the inverse $\mathbf{D}^{-1}$ of the unitary matrix $\mathbf{D}$ is the transpose of its complex conjugate matrix;

$$\mathbf{D}^{-1} = (\mathbf{D}^*)^T = \mathbf{D}^\dagger, \tag{53}$$

where $\mathbf{D}^\dagger$ is a commonly used alternative notation. The columns of the transformation matrix contain the eigenvectors of $\mathbf{A}$. This can be seen by multiplying Eq. (52) with $\mathbf{D}$ from the left, giving

$$\mathbf{A}\mathbf{D} = \mathbf{D}\mathbf{E}. \tag{54}$$

Since $\mathbf{E}$ is diagonal, the nth column of $\mathbf{D}$ on the right side is multiplied by the nth eigenvalue (i.e., the matrix element E_{nn}). On the left multiplication by $\mathbf{A}$, the nth column of $\mathbf{D}$ gives the nth column of $\mathbf{A}\mathbf{D}$, i.e.,

$$\mathbf{A}\mathbf{D}_n = E_{nn}\mathbf{D}_n, \tag{55}$$

and thus $\mathbf{v}_n = \mathbf{D}_n$.

The number of operations needed to diagonalize an $N \times N$ matrix generally scales as N^3, which, along with memory requirements for storing the matrix, limits the size of matrices that can be diagonalized in practices. Currently, N of the order of $1000 - 2000$ can be handled without too much effort on a desktop computer.

Many linear algebra books discuss matrix diagonalization in detail (*Numerical Recipes* does as well), and we shall not go into this subject of numerical analysis here. In practice, it is advisable to use "canned" subroutines for diagonalization. A useful on-line resource is `gams.nist.gov`, which contains a large number of diagonalization routines for different types of matrices (general real or complex, symmetric, hermitean, sparse, etc.). On the course web site, some useful Fortran 77 routines from the LAPACK library are available, along with simplified Fortran 90 interface subroutines.

3.4 One-dimensional example

Although the utility of variational methods is primarily in higher-dimensional problems, we will here consider an illustrative example in one dimension. The generalizations to two- and three-dimensional problems are obvious.
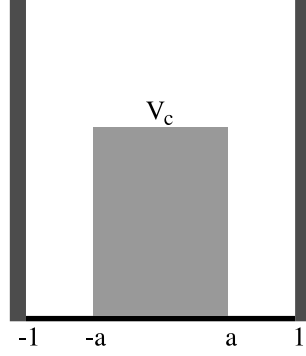
Figure 4: Square-well potential with an internal barrier of height V_c

For the square well potential with infinite barriers at $x = \pm 1$, the eigenfunctions are (with $\hbar = m = 1$)

$$\phi_k(x) = \begin{cases} \cos(k\pi x/2), & \text{for odd } k, \\ \sin(k\pi x/2), & \text{even odd } k, \end{cases} \tag{56}$$

and the corresponding energy eigenvalues are

$$K_k = \frac{1}{8}k^2\pi^2, \tag{57}$$

where we use K to indicate that this energy is purely kinetic. Any wave function $\Psi(x)$ in the range $[-1, 1]$ with boundary conditions $\Psi(\pm 1) = 0$ can be expanded using these states as basis states. A variational calculation can hence be carried out in this basis, truncated at $k = N$, for any form of the potential between $x = -1$ and 1. Here we consider a square potential barrier of height V_c between $x = -a$ and a, as illustrated in Fig. 4. The Hamiltonian matrix elements are

$$H_{pk} = \langle p|(-\frac{1}{2}\frac{d^2}{dx^2} + V)|k\rangle = K_k + V_c \int_{-a}^{a} dx \phi_p(x)\phi_k(x). \tag{58}$$

In this case the potential-energy matrix elements can be easily calculated analytically, whereas in general they would have to be evaluated using numerical integration.

A program carrying out this variational calculation is available on the course web site, in the file 'sqvar.f90' (which should be compiled with the supplied LAPACK diagonalization routine DSYEV in the file 'dsyev.f'). In order for this program to be easily adapted also for other types of potentials inside the square well, the integrals in (58) are calculated numerically, using a Romberg algorithm.

We here discuss results for $V_c = 10$, for which the ground state energy calculated using Numerov's integration scheme is $E_0 = 7.76056$. Using the variational method with increasing number of basis states gives $E_0 = 9.41680$ ($N = 1$), 7.798175 ($N = 3$), 7.79671 ($N = 5$), 7.78016 ($N = 7$),...,7.76062 ($N = 50$). For this symmetric potential, only odd-numbered states contribute to the ground state. Some of the resulting ground state wave functions are shown along with the numerically exact solution in Fig. 5. Note that for $N = 1$ the wave function is the same as for the pure square-well potential, and the energy corresponds to that of first-order perturbation theory. Clearly the variational calculation performs very well in this case, with already $N = 9$ giving the ground state energy to one part in 1000 and a wave function almost indistinguishable from the exact solution. If we make the barrier V_c larger, the convergence of the variational calculation becomes worse, as more states are needed to form a wave function which is very small in the range $[-a, a]$.
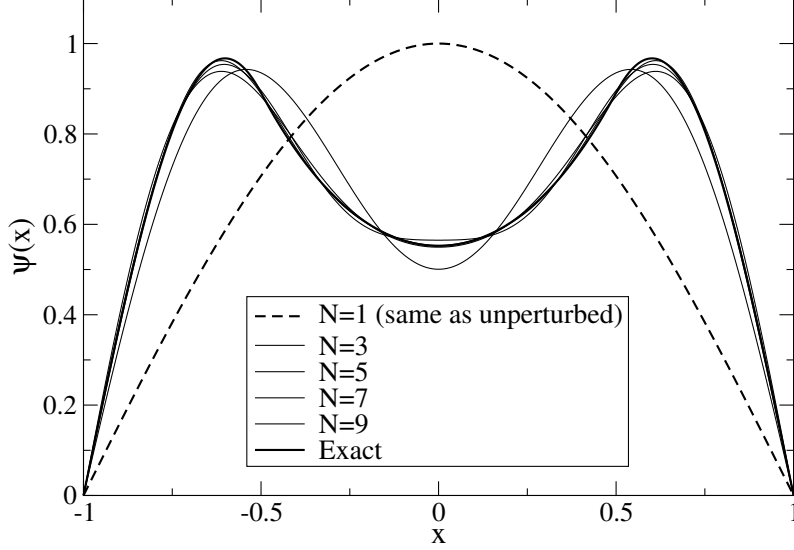
12

Figure 5: Variational wave functions for the square-well potential with an internal barrier of height $V_c = 10$ for different basis sizes N.

3.5 Variational calculations with non-orthogonal states

If we use a set of non-orthogonal wave functions in a variational calculation, it is not immidiately clear how we should proceed. We therefore have to generalize the calculation of the leading-order energy shift carried out in Sec. 3.2, in order to see what conditions arise when this shift is set to zero. The only difference is that the scalar product of orthonormal states, $\langle p|k \rangle = \delta_{pk}$, has to be replaced by a non-diagonal overlap matrix;

$$\langle p|k \rangle = \int dx^d \phi_p^*(\vec{x}) \phi_k(\vec{x}) \equiv W_{pk}. \tag{59}$$

The energy functional is then

$$E = \frac{\langle \Psi|H|\Psi \rangle}{\langle \Psi|\Psi \rangle} = \frac{\sum_{kp} C_k C_p^* H_{kp}}{\sum_{kp} C_k C_p^* W_{kp}}. \tag{60}$$

Proceding as in Eq. (46), by making a small change δ_q in the coefficient C_q, the energy to leading order in δ_q is found to be

$$E(\delta_q) = \left(E + \frac{\sum_k (C_k \delta_q^* H_{qk} + \delta_q C_k^* H_{kq})}{\sum_{kp} C_k C_p^* W_{kp}} \right) \left(1 - \frac{\sum_k (C_k \delta_q^* W_{qk} + \delta_q C_k^* W_{kq})}{\sum_{kp} C_k C_p^* W_{kp}} \right). \tag{61}$$

From this we get the shift

$$E(\delta_q) - E = \frac{\sum_k (C_k \delta_q^* H_{qk} + \delta_q C_k^* H_{kq})}{\sum_{kp} C_k C_p^* W_{kp}} - E \frac{\sum_k (C_k \delta_q^* W_{qk} + \delta_q C_k^* W_{kq})}{\sum_{kp} C_k C_p^* W_{kp}}, \tag{62}$$

and for this to vanish we must have

$$\sum_k (\delta_q^* C_k H_{qk} + \delta_q C_k^* H_{kq}) = E \sum_k (\delta_q^* C_k W_{qk} + \delta_q C_k^* W_{kq}). \tag{63}$$

13

As before, the terms containing δ_q and δ_q^* correspond to exactly the same condition on the coefficients C_k, giving, for each $q = 1, \ldots, N$,

$$\sum_k C_k H_{qk} = E \sum_k C_k W_{qk}, \tag{64}$$

which is equivalent to the matrix equation

$$\begin{pmatrix} H_{11} & H_{12} & \cdots & H_{1N} \\ H_{21} & H_{22} & \cdots & H_{2N} \\ \vdots & & \ddots & \vdots \\ H_{N1} & H_{N2} & \cdots & H_{NN} \end{pmatrix} \begin{pmatrix} C_1 \\ C_2 \\ \vdots \\ C_N \end{pmatrix} = E \begin{pmatrix} W_{11} & W_{12} & \cdots & W_{1N} \\ W_{21} & W_{22} & \cdots & W_{2N} \\ \vdots & & \ddots & \vdots \\ W_{N1} & W_{N2} & \cdots & W_{NN} \end{pmatrix} \begin{pmatrix} C_1 \\ C_2 \\ \vdots \\ C_N \end{pmatrix}, \tag{65}$$

or, in more compact notation,

$$\mathbf{HC} = E\mathbf{WC}. \tag{66}$$

This is called a generalized eigenvalue problem. It can be solved using matrix diagonalization if the overlap matrix $\mathbf{W}$ can first be transformed into a unit matrix;

$$\bar{\mathbf{B}}^{-1}\mathbf{W}\bar{\mathbf{B}} = \mathbf{I}. \tag{67}$$

This can be done by first diagonalizing $\mathbf{W}$. We denote by $\mathbf{B}$ the unitary transformation that diagonalizes $\mathbf{W}$, leading to an eigenvalue matrix $\mathbf{W_d}$;

$$\mathbf{B}^{-1}\mathbf{W}\mathbf{B} = \mathbf{W_d}. \tag{68}$$

If all the eigenvalues are positive, a transformation to the unit operator can now be easily constructed using the inverse square root of the eigenvalue matrix:

$$\mathbf{W_d}^{-1/2}\mathbf{B^{-1}}\mathbf{W}\mathbf{B}\mathbf{W_d}^{-1/2} = \mathbf{I}. \tag{69}$$

The desired tranformation matrix is thus

$$\bar{\mathbf{B}} = \mathbf{B}\mathbf{W_d}^{-1/2}. \tag{70}$$

It can be proven that in fact the overlap matrix has only positive eigenvalues, and this procedure can hence be carried out. We can then rewrite the generalized eigenvalue problem (66) as follows;

$$\bar{\mathbf{B}}^{-1}\mathbf{H}\bar{\mathbf{B}}\bar{\mathbf{B}}^{-1}\mathbf{C} = E\bar{\mathbf{B}}^{-1}\mathbf{W}\bar{\mathbf{B}}\bar{\mathbf{B}}^{-1}\mathbf{C}. \tag{71}$$

Using the definitions,

$$\mathbf{H_B} = \bar{\mathbf{B}}^{-1}\mathbf{H}\bar{\mathbf{B}}, \tag{72}$$
$$\mathbf{C_B} = \bar{\mathbf{B}}^{-1}\mathbf{C}, \tag{73}$$

we have thus constructed a standard eigenvalue problem;

$$\mathbf{H_B}\mathbf{C_B} = E\mathbf{C_B}. \tag{74}$$

When this has been solved we can obtain the eigenvectors of the original equation (66) from Eq. (73);
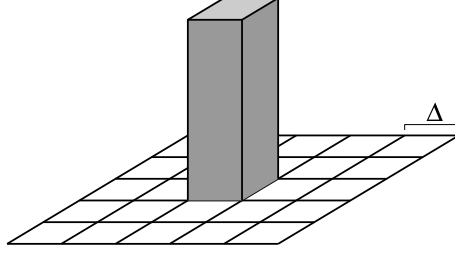$\mathbf{C} = \bar{\mathbf{B}}^{-1}\mathbf{C_B}$.

Figure 6: A basis function $\phi_i(\vec{x})$ localized inside a square element of a two-dimensional space. The height of the normalized function is $\Delta^{-1/2}$.

4 The Schrödinger equation in discretized space

As an example of a grid-based method for solving the Schrödinger equation in any number of dimensions, we will here develop the simplest way to discretize the equation in real space. The method can technically be considered a linear variational method, in a space of basis functions describing particles localized in a finite region of space. Typically the number N of such basis functions must be very large in $d = 2$ and 3, and hence it may not be possible in practice to completely diagonalize the resulting Hamiltonian matrix. We will therefore introduce the so-called Lanczos diagonalization method, with which one can easily obtain the ground state and a number of excited states also for very large basis sets (millions, or even tens of millions of states).

4.1 Discrete real-space Hamiltonian

For a d-dimensional space, we subdivide the volume in which the Schrödinger equation is to be solved into cubic elements of linear size Δ, i.e., with volume Δ^d. We can label the elements by d-component vectorz corresponding to their actual coordinates, or just use single integers assigned to the elements in some suitable manner. To simplify the notation, we will here use integers $j = 0, 1, \ldots$ for the labels and denote the coordinate of the center of the jth element $\vec{r}_j$. The basis states are denoted $|j\rangle$ and the corresponding wave functions $\phi_j(\vec{x})$.

The basis functions are taken to be constant within their respective elements i and zero elsewhere. Normalization then requires that the constant value is $\Delta^{-d/2}$, i.e.,

$$\phi_j(\vec{x}) = \begin{cases} \Delta^{-d/2}, & \text{if } -\frac{\Delta}{2} \leq (\vec{x} - \vec{r}_j)_\alpha < \frac{\Delta}{2}, \quad \alpha = 1, ..., d, \\ 0, & \text{else}, \end{cases} \tag{75}$$

where $()\alpha$ denotes a component of the vector inside the parentheses. Such a basis function in two dimensions is illustrated in Fig. 6. Clearly different states do not overlap, $\langle j|l\rangle = \delta_{jl}$, and the basis is orthonormal. One might worry that, strictly speaking, the basis functions are not valid wave functions, since they are discontinuous. However, what matters is that we obtain a scheme that reproduces the correct physics as the discretization $\Delta \to 0$, which we will prove is indeed the case.

In a cubic box with volyme L^3, the size of the basis is $N = (L/\Delta)^d$; we assume that L is a multiple of Δ. We now proceed to calculate the matrix elements of the Hamiltonian, $H = K + V$, in this

discrete basis. The potential energy V is diagonal;

$$V_{jl} = \langle j|V|l \rangle = \delta_{jl} \int dx^d |\phi_j(\vec{x})|^2 V(\vec{x}), \tag{76}$$

which we can also approximate by

$$V_{jl} \approx \delta_{jl} V(\vec{r}_j). \tag{77}$$

Looking at the matrix element of the kinetic energy (with $\hbar = m = 1$),

$$K_{jl} = \langle j|K|l \rangle = \frac{1}{2} \int dx^d \phi_j(\vec{x}) \nabla^2 \phi_l(\vec{x}), \tag{78}$$

we are directly faced with the fact that the basis functions are not differentiable. How can we proceed then? We will use the central difference operator definition of the second derivative, e.g., in one dimension we will replace the second derivative by

$$\frac{1}{\Delta^2} \delta^2 \phi_j(x) = \frac{1}{\Delta^2} [\phi_j(x - \Delta) - 2\phi_j(x) + \phi_j(x + \Delta)]. \tag{79}$$

This approach can clearly also be criticized based on the fact that the function $\phi_j(x)$ is not slowly varying, but, again, we will show that in fact correct results are obtained as $\Delta \to 0$. Acting on $\phi_l(x)$, the central difference operator above gives $\frac{1}{2}\Delta^{-5/2}$ for $x \in [r_l - 3\Delta/2, r_l - \Delta/2]$ and $x \in [r_l + \Delta/2, r_l + 3\Delta/2]$ and $\Delta^{-5/2}$ for $x \in [r_l - \Delta/2, r_l + \Delta/2]$, as illustrated in Fig. 7. In the integral in Eq. (78), ϕ_j gives a factor $\Delta_{-1/2}$ and the integral over the individual x ranges above gives a factor Δ. Thus

$$K_{jl} = \frac{1}{2} \int dx^d \phi_j(\vec{x}) \frac{1}{\Delta^2} \delta^2 \phi_l(\vec{x}) = \begin{cases} -\Delta^{-2}/2, & \text{for } j = l \pm 1, \\ \Delta^{-2}, & \text{for } j = l. \end{cases} \tag{80}$$

The action of the kinetic energy on a basis state hence leads to

$$K|j\rangle = -\frac{1}{\Delta^2} \left[\frac{1}{2}|j-1\rangle - |j\rangle + \frac{1}{2}|j+1\rangle \right], \tag{81}$$

and the non-zero matrix elements of the full Hamiltonian are, using Eq. (77),

$$H_{j,j} = V(r_j) + \frac{1}{\Delta^2}, \tag{82}$$

$$H_{j\pm1,j} = -\frac{1}{2}\frac{1}{\Delta^2}. \tag{83}$$

This result generalizes to two and thre dimensions. Denoting by $\delta[j]$ an element neighboring j, of which there are four in 2D and six in 3D, the action of the Hamiltonian on a basis state results in

$$H|j\rangle = \left(V(r_j) + \frac{d}{\Delta^2} \right)|j\rangle - \frac{1}{2}\frac{1}{\Delta^2} \sum_{\delta[j]} |\delta[j]\rangle, \tag{84}$$

and hence the matrix elements are

$$H_{j,j} = V(\vec{r}_j) + \frac{d}{\Delta^2}, \tag{85}$$

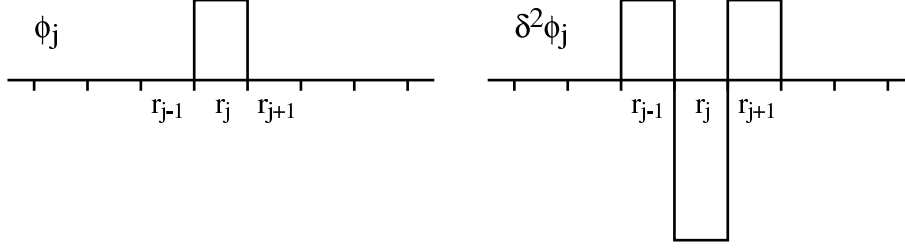$$H_{\delta[j],j} = -\frac{1}{2}\frac{1}{\Delta^2}. \tag{86}$$

16

Figure 7: A one-dimensional basis function (left) and its discrete second derivative (right).

To prove that the discretized Hamiltonian reproduces the correct physics as $\Delta \to 0$, we consider a free particle, i.e., $V = 0$ (only the kinetic energy was subjecy to suspect manipulations above, and hence we only need to investigate it). We will first diagonalize the Hamiltonian in one dimension. In continuum space, for a finite periodic system of length L, the energy eigen functions are $\phi_k(x) = \exp(-ikx)$, with $k = n2\pi/L$, $n = 0, 1. \ldots$. In the discretized box with $N = L/\Delta$ elements, we will show that the eigenstates are

$$|k\rangle = \frac{1}{\sqrt{N}} \sum_{j=0}^{N-1} e^{-ikr_j} |j\rangle, \quad k = n2\pi/L, \quad 0, 1, \ldots, N-1, \tag{87}$$

where k only takes N different values because for the discrete coordinates $r_j = j\Delta = jL/N$ we have $\exp[-i(n+N)2(\pi/L)r_j] = \exp[-in2(\pi/L)r_j]$, i.e., $|k + N2\pi/L\rangle = |k\rangle$. Acting with the kinetic energy operator on the proposed state (87) gives, using Eq. (81),

$$K|k\rangle = -\frac{1}{\Delta^2} \frac{1}{\sqrt{N}} \sum_{j=0}^{N} e^{-ikr_j} \left[\frac{1}{2}|j-1\rangle - |j\rangle + \frac{1}{2}|j+1\rangle \right]. \tag{88}$$

By shifting the indexes in the $j \pm 1$ terms by ± 1 and using the periodic boundary conditions, $|j = N + 1\rangle = |j = 1\rangle$ and $|j = -1\rangle = |j = N\rangle$, we can rewrite this as

$$K|k\rangle = -\frac{1}{\Delta^2} \frac{1}{\sqrt{N}} \sum_{j=0}^{N} e^{-ikr_j} \left[\frac{1}{2}(e^{ik\Delta} + e^{-ik\Delta}) - 1 \right] |j\rangle = -\frac{1}{\Delta^2}[\cos(k\Delta) - 1]|k\rangle, \tag{89}$$

and hence the energy eigenvalues are

$$E_k = \frac{1}{\Delta^2}[1 - \cos(k\Delta)]. \tag{90}$$

For small $k\Delta$, we can Taylor expand the cosine;

$$E_k = \frac{1}{2}k^2 - \frac{1}{24}\Delta^2 k^4 + \ldots, \tag{91}$$

which agrees with the energy of the free particle in the continuum, $E_k = k^2/2$, to leading order. This proves that the discretized scheme is valid. Note that the correction to the energy is negative, and hence although the way the discrete basis was introduced corresponds to a variational method, the errors introduced in discretizing the kinetic energy operator has resulted in a correction with

17

a sign different from purely variational schemes. In three dimensions the above energy calculation easily generalizes to

$$E_k = \frac{1}{\Delta^2}[3 - \cos(k_x\Delta) - \cos(k_y\Delta) - \cos(k_z\Delta)], \tag{92}$$

which again agrees with the continuum result up to a negative fourth-order correction.

It can here be noted that in solid-state physics a discrete space arises naturally in a crystal structure. The coordinates $\vec{r}_j$ above then represent the locations of the atoms on a lattice (which of course can be any type of crystal lattice). In weakly overlapping valence-electron orbitals, the electrns are almost localized at the individual atoms. Orthogonal states, so-called *Wannier states*, can be constructed and are also highly localized if the original atomic orbitals are weakly overlapping. With these basis states the kinetic energy takes exactly the form derived above, with the factor $1/\Delta^2$ replaced by a *hopping matrix element* t_{ij} between orbitals i and j, which depends on the details of the Wannier orbitals. In the *tight binding* approximation, only short-range hopping matrix elements are taken into account (not necessarily only between nearest neighbors, however). This is often a good approximation for materials with partially filled d and f orbitals, in particular. The tight-binding approach forms the basis of many calculations that include also electron-electron interactions.

4.2   The Lanczos diagonalization method

Although the size of the $N \times N$ Hamiltonian matrix in discretized space is very large in two and three dimensions, the number of non-zero matrix elements is much smaller; on the order of the number of states N. There are sveral efficient methods available for treating such *sparse* matrices. Here we shall discuss the perhaps most well known of them—the *Lanczos method*. This approach gives systematically controllable approximations for low and high eigenvalues eigenvalues (of which we are typically only interested in the low ones) and the corresponding eigenstates. The Lanczos method is based on a particular transformation which brings the Hamiltonian into a tridiagonal form (i.e., with non-zero matrix elements only on the diagonal and the two "subdiagonals" on either side of the diagonal).

The basic idea of the Lanczos method, or, more generally, *Krylov space methods*, is the following: Consider an arbitrary state $|\Psi\rangle$ and its expansion in terms the eigenstates $\Psi_k\rangle$ of the Hamiltonian. We operate with a power of the Hamiltonian on the state;

$$H^m|\Psi\rangle = \sum_k C_k E_k^m |\Psi_k\rangle. \tag{93}$$

If the power m is large, the state k with the largest absolut value $|E_k|$ of the energy will dominate the sum, provided that the corresponding expansion coefficient $C_k \neq 0$. Hence, the process of acting many times with the Hamiltonian on a state will project out either the state with the smallest or the largest eigenvalue. If we want to make sure that the ground state is obtained (for $m \to \infty$, or an approximation to the ground state for finite m), we can instead act with $(H - \sigma)^m$, where σ is a positive number large enough to make $|E_0 - \sigma|$ larger than $|E_{\max} - \sigma|$, where $E_{\max}$ is the highest eigenvalue of H.

The state $(H - \sigma)^m|\Psi\rangle$ is a certain linear combination of states $H^m|\Psi\rangle$ $m = 0, 1., \ldots, n$. A more efficient way to construct a state approaching the ground state as $m \to \infty$ is to diagonalize the

Hamiltonian in a basis spanned by all these states $H^m|\Psi\rangle$ constructed one by one by successive operations with H. In this space a better linear combination for minimizing the energy typically exists, and, as we showed in Sec. 3.2, the way to find it is to diagonalize H in the finite basis. In addition to the ground state, this approach also can give low-lying excited states.

The subspace of states obtained by acting multiple times with the Hamiltobian on a state is called the Krylov space. We are here discussing Hamiltonians in quantum mechanics, but Krylov space methods of course apply to eigenvalue problems more generally as well, and are very widely used in many areas of science and engineering.

The Lanczos method amounts to constructing orthogonal basis states that are linear combinations of the Krylov space states in such a way that the Hamiltonian written in this basis is tridiagonal. A basis $\{|f_n\rangle\}$ is first constructed that is orhogonal but not normalized, and subsequently from these states an orthonormal set $\{|\phi_n\rangle\}$ is obtained. The basis construction starts from an arbitrary normalized state $|f_0\rangle$, of which is required only that it is not orthogonal to the ground state of H (if the goal of the calculation is to find the ground state). The next state is given by

$$|f_1\rangle = H|f_0\rangle - a_0|f_0\rangle, \tag{94}$$

where the constant a_0 is to be chosen such that $|f_1\rangle$ is orthogonal to $|f_0\rangle$. The overlap between the two states is

$$\langle f_1|f_0\rangle = \langle f_0|H|f_0\rangle - a_0\langle f_0|f_0\rangle = H_{00} - a_0 N_0, \tag{95}$$

where $N_0 = 1$ is the normalization of $|f_0\rangle$. Hence, for the overlap to vanish we must have

$$a_0 = H_{00}/N_0. \tag{96}$$

The next state is written as

$$|f_2\rangle = H|f_1\rangle - a_1|f_1\rangle - b_0|f_0\rangle, \tag{97}$$

where a_1 and b_0 are to be chosen in such a way that $|f_2\rangle$ is orthogonal to both the previous states. Calculating the overlaps, using the expression for $H|f_0\rangle$ and $H|f_1\rangle$ obtained from Eqs. (94) and (97),

$$
\begin{aligned}
\langle f_2|f_1\rangle &= \langle f_1|H|f_1\rangle - a_1\langle f_1|f_1\rangle - b_0\langle f_0|f_1\rangle \\
&= H_{11} - a_1 N_1, \tag{98} \\
\langle f_2|f_0\rangle &= \langle f_1|H|f_0\rangle - a_1\langle f_1|f_0\rangle - b_0\langle f_0|f_0\rangle \\
&= \langle f_1|f_1\rangle + a_0\langle f_1|f_0\rangle - b_0 N_0 \\
&= N_1 - b_0 N_0, \tag{99}
\end{aligned}
$$

shows that the coefficients are given by

$$
\begin{aligned}
a_1 &= H_{11}/N_1, \tag{100} \\
b_0 &= N_1/N_0. \tag{101}
\end{aligned}
$$

For general n, Eq. (97) generalizes to

$$|f_{n+1}\rangle = H|f_n\rangle - a_n|f_n\rangle - b_{n-1}|f_{n-1}\rangle, \tag{102}$$

and the coefficients making this state orthogonal to $|f_n\rangle$ and $|f_{n-1}\rangle$ are

$$
\begin{align}
a_n &= H_{nn}/N_n, \tag{103}\\
b_{n-1} &= N_n/N_{n-1}. \tag{104}
\end{align}
$$

It remains to show that with these coefficients the state $|f_{n+1}\rangle$ is orthogonal also to all states $|f_k\rangle$ with $k < n - 1$. We begin with $n + 1 = 3$, for which the overlap with $f_0\rangle$ is

$$
\langle f_3|f_0\rangle = \langle f_2|H|f_0\rangle - a_2\langle f_2|f_0\rangle - b_1\langle f_1|f_0\rangle = \langle f_2|f_1\rangle + a_0\langle f_2|f_0\rangle = 0. \tag{105}
$$

For successively higher $n + 1$, we can now use the fact that all previously generated states are orthogonal to obtain, using also $H|f_n\rangle$ given by Eq. (102),

$$
\begin{align}
\langle f_{n+1}|f_{n-k}\rangle &= \langle f_n|H|f_{n-k}\rangle - a_n\langle f_n|f_{n-k}\rangle - b_{n-1}\langle f_{n-1}|f_{n-k}\rangle \\
&= \langle f_n|f_{n-k+1}\rangle + a_{n-k}\langle f_n|f_{n-k}\rangle + b_{n-k-1}\langle f_n|f_{n-k-1}\rangle \tag{106}\\
&= 0.
\end{align}
$$

This basis is thus indeed orhogonal.

To write the Hamiltonian in the basis $\{|f_n\rangle\}$ we use the expression for the Hamiltonian acting on one of the basis states, obtained from Eq. (102);

$$
H|f_n\rangle = |f_{n+1}\rangle + a_n|f_n\rangle + b_{n-1}|f_{n-1}\rangle, \tag{107}
$$

and thus the non-zero matrix elements are

$$
\begin{align}
\langle f_{n-1}|H|f_n\rangle &= b_{n-1}N_{n-1} = N_n, \\
\langle f_n|H|f_n\rangle &= a_nN_n, \tag{108}\\
\langle f_{n+1}|H|f_n\rangle &= N_{n+1}.
\end{align}
$$

The normalized basis states are

$$
|\phi_n\rangle = \frac{1}{\sqrt{N_n}}|f_n\rangle. \tag{109}
$$

Recalling that $b_n = N_{n+1}/N_n$, the non-zero matrix elements in the orthonormal basis are

$$
\begin{align}
\langle \phi_{n-1}|H|\phi_n\rangle &= \sqrt{b_{n-1}}, \\
\langle \phi_n|H|\phi_n\rangle &= a_n, \tag{110}\\
\langle \phi_{n+1}|H|\phi_n\rangle &= \sqrt{b_n}.
\end{align}
$$

This is a tri-diagonal matrix, which can be diagonalized using special methods that are faster than a generic exact diagonalization. The main advantage of a tri-diagonal matrix is not, however, that it can be diagonalized more easily, but that it can be constructed quickly. The Lanczos method is advantageous in practice only if the ground state can be reproduced using a basis size M that is significantly smaller than the size of the full Hilbert space. This is often the case, and one can then obtain the ground state (and some times excited states) in cases where a complete diagonalization of the Hamiltonian in the original basis would be impossible.

One thing to be noted is that the Lanczos method cannot produce several degenerate states; out of a degenerate set of states, only a particular linear combination of them will be obtained (which

13	14	15	16
9	10	11	12
5	6	7	8
1	2	3	4

Figure 8: Example of labeling of the volume elements of an $L \times L$ lattice, here with $L = 4$.

depends on the initial state $f_0\rangle$). To see the reason for this, we again look at the expansion (93) of a state $H^m|\Psi\rangle$, in which we assume that there are two degenerate states $|\Psi_i\rangle$ and $|\Psi_j\rangle$ that we have isolated from the rest of the sum;

$$H^m|\Psi\rangle = \sum_{k=\neq i,j} C_k E_k^m|\Psi_k\rangle + E_j^m(C_i|\Psi_i\rangle + C_j|\Psi_j\rangle). \tag{111}$$

Here it is evident that for any m, the expansion will contain the same linear combination of the states $|\Psi_j\rangle$ and $|\Psi_j\rangle$. Hence, in a subspace spanned by the set of states $H^n|\Psi\rangle$, $n = 0, \ldots, M-1$, there is no freedom in obtaining different linear combinations of the two degenerate states. This of course generalizes to degenerate multiplets with more than two states.

4.3   Programming the Lanczos algorithm

The most critical aspect of generating the Lanczos basis is the operation with the Hamiltonian on a basis state $|f_n\rangle$, which is done component-wise according to (84), to obtain the following state $|f_{n+1}\rangle$ as prescribed in Eq. (102). For the kinetic part, we need to be able to rapidly find all the neighbors $\delta[j]$ of a given volume element j. The neighbors can be stored in a pre-generated table, but for simple geometries it is also very easy to find the neighbors on the fly (this is often faster in practice, since less memory access is required). With the labeling scheme $j = x + (y-1)L_x$, illustrated for $L \times L$ elements with $L = 4$ in Fig. 8, the neighbors of internal elements can be obtained by adding or subtracing 1 or L for neigbors in the x and y direction, respectively. Elements on the boundaries need special, but simple, considerations which depend on the type of boundary conditions used (open or periodic).

Considering a two-dimensional case, a rectangular open-boundary system with $L_x \times L_y$ elements, this is the main part of a Fortran 90 subroutine taking a state stored in a vector `f1(lx*ly)` as input and giving the state when the Hamiltonian has acted on it in the vector `f2(lx*ly)`:

```
subroutine hoperation(lx,ly,f1,f2)
f2=potential*f1
do j=1,lx*ly
   x=1+mod(j-1,lx)
   y=1+(j-1)/lx
   if (x /= 1) f2(j)=f2(j)-thop*f1(j-1)
   if (x /= lx) f2(j)=f2(j)-thop*f1(j+1)
   if (y /= 1) f2(j)=f2(j)-thop*f1(j-lx)
   if (y /= ly) f2(j)=f2(j)-thop*f1(j+lx)
end do
```

Here the potential energy is stored in the vector `potential(lx*ly)` and `thop` is the kinetic prefactor $1/2\Delta^2$. For the open-boundary system, the hopping processes corresponding to going outside the system boundaries are suppressed; this is equivalent to having infinitely repulsive walls.

Using the subroutine `hoperation`, the construction of the Hamiltonian, i.e., the coefficients a_i and b_i, in a Lanczos basis of size M can be done with the following code:

```
f0=psi0
nn(0)=1.d0
call hoperation(lx,ly,f0,f1)
aa(0)=dot_product(f0,f1)
f1=f1-aa(0)*f0
nn(1)=dot_product(f1,f1)
do i=2,m
  call hoperation(lx,ly,f1,f2)
  aa(iter-1)=dot_product(f1,f2)/nn(iter-1)
  bb(iter-2)=nn(iter-1)/nn(iter-2)
  f2=f2-aa(iter-1)*f1-bb(iter-2)*f0
  nn(iter)=dot_product(f2,f2)
  f0=f1; f1=f2
end do
```

Here an initial state has been prepared in the vector `psi0`, and the coefficients a_i,b_i and the normalizations N_i are stored in vectors `aa(0:m)`, `bb(0:m)`, and `nn(0:m)`, respectively. Scalar products are calculated using the Fortran 90 intrinsic function `dot_product`.

The diagonalization of the tridiagonal matrix, the diagonal elements of which are in the vector `aa` and the two subdiagonals of which are given by `sqrt(bb)`, can be done using special techniques for tridiagonal matrices. The LAPACK Fortran 77 tridiagonal diagonalization routine DSTEV is available on the course web-site, along with a simplified Fortran 90 interface subroutine. Based on the transformation matrix obtained as output in such a diagonalization, we can construct the eigenstates. However, in the procedures above we have not stored all the states $|f_n\rangle$, since this would typically demand too much memory, and hence we need to reconstruct these states in order to be able to find the eigenstates. The Lanczos procedure typically gives good results only for a few low-lying states, and hence one would typically only want to construct one or a few states. If we have stored the kth column of the transformation matrix, corresponding to the kth eigenstate, in a vector `vec(0:m-1)`, we can carry out the transformation of the states $|f_n\rangle$ to the desired eigenstate as follows:

```
f0=psi
psi=vec(0)*psi
call hoperation(lx,ly,f0,f1)
f1=f1-aa(0)*f0
psi=psi+vec(1)*f1/sqrt(nn(1))
do i=2,m-1
  call hoperation(lx,ly,f1,f2)
  f2=f2-aa(i-1)*f1-bb(i-2)*f0
```

M	E_0	E_1	E_2
10	165.47488	1116.18787	3077.75501
20	36.464497	268.910471	744.48445
30	15.339143	155.724962	332.96633
50	9.172055	47.562526	146.64266
100	1.696802	12.229263	27.56645
150	1.262146	10.191426	14.60174
160	1.234164	6.045649	11.09876
170	1.224724	5.160069	11.01756
180	1.222428	4.974962	11.00148
190	1.221635	4.905657	10.99395
200	1.221430	4.885423	10.99108
Exact	1.233701	4.934802	11.10330

Table 1: The three lowest energy eigenvalues for different basis sizes M in Lanczos calculations for a one-dimensional hard-wall box of length 2, using discretization $\Delta = 0.01$.

```
   psi=psi+vec(i)*f2/sqrt(nn(i))
   f0=f1; f1=f2
end do
```

Here `psi(lx*ly)` initially contains the original state that was previously used to start the construction of the Lanczos Hamiltonian. It is now used also to hold the eigen vector.

4.4   Examples

We first consider a one-dimensional example; a particle-in-a-box potential with hard walls at $x = \pm 1$. Table 1 shows the three lowest energy eigenvalues for different Lanczos basis sizes M in a calculation with $\Delta = 0.01$, i.e., discretization of the system into 200 volume elements. For small M, the energies are much too large, reflecting the high energy of the initial random state. The energies come close to the exact values only when M approaches the number of volume elements. Due to the discretization, we do not obtain the exact energy; in accordance with Eq. (91) the energy of the discretized system is lower than the exact value. The wave functions corresponding to the lowest eigenvalue in the calculations with $M = 50, 100$, and 200 are shown in Fig. 9. At $M = 150$ the wave function is still far from the exact particle-in-a-box ground state, $\Psi_0(x) = \cos(\pi x/2)$, but at $M = 200$ this function is well approximated.

The above example illustrates the fact that the Lanczos method does not work well for solving the discretized Schrödinger equation in one dimension, since a basis set reduction relative to the full Hilbert space is not achieved. In one dimension there are in any case more accurate and practical methods available, e.g., the Numerov differential equation solver discussed in Sec. 2.1.

The reason why the Lanczos method fails for the one-dimensional discretized Schrödinger equation is that a state $H^m|\psi\rangle$ is a linear combination of states that differ from $|\Psi\rangle$ in at most m real-space basis expansion coefficients, corresponding to a contiguous segment of m system elements.
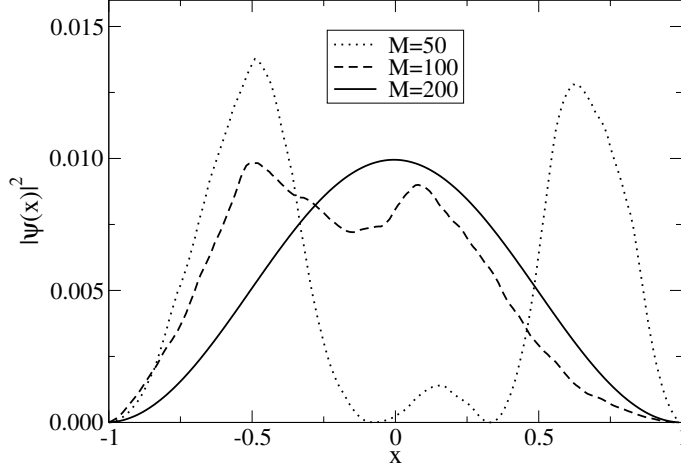
Figure 9: Wave function squared obtained in Lanczos calculations with different basis sizes M for a one-dimensional hard-wall potential discretized using 200 elements ($\Delta = 0.01$). The initial state was the same randomly generated state in all cases.
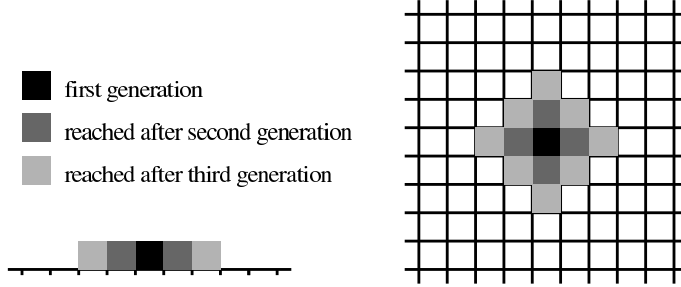

Figure 10: Basis states that can have non-zero weight in a Lanczos basis after $n = 0, 1, 2$ steps (first, second, and third generation of states) when the initial state consists of a single basis vector, indicated by a black square, in one dimension (left) and two dimensions (right).

Starting from an arbitrary state, we would expect to be able to construct a good approximation to an eigenstate only if we can mix states that have different weights for basis states all through the system, which would require m to be equal to the number of discretization elements L/Δ, in accord with what we observed in the example above. In two and three dimensions the method can be expected to work better, because although $H^m|\psi\rangle$ still only can mix states that differ by m expansion coefficients, these coefficients can form paths that span across the whole system if m is of the order of the linear number of elements L/Δ, i.e., the square or cubic root of the total number of elements, not the total number of elements $(L/\Delta)^d$.

The above arguments are illustrated in Fig. 10, which shows a 1D and a 2D system in which the starting state is a single basis vector; $|\psi\rangle = |j\rangle$. The basis vectors that can have non-zero weight in $H^n|\Psi\rangle$ after two and three "generations" ($n = 1, 2$) are shown. Clearly, an eigenstate of the system would in general have non-zero weight for all basis vectors, and this would require $n \sim L/\Delta$ in both cases. We would hence expect convergence with a Lanczos basis of size $M \sim L/\Delta$ in any number of dimensions, and hence a larger comparative advantage of the Lanczos method in higher dimensions.
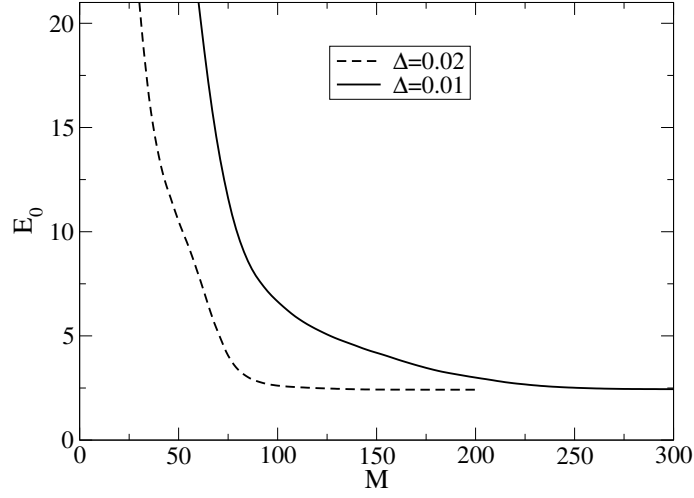
24

Figure 11: Ground state energy as a function of the Lanczos basis size for a two-dimensional hard-wall box of size 2×2. Results for two different discretizations Δ are shown.
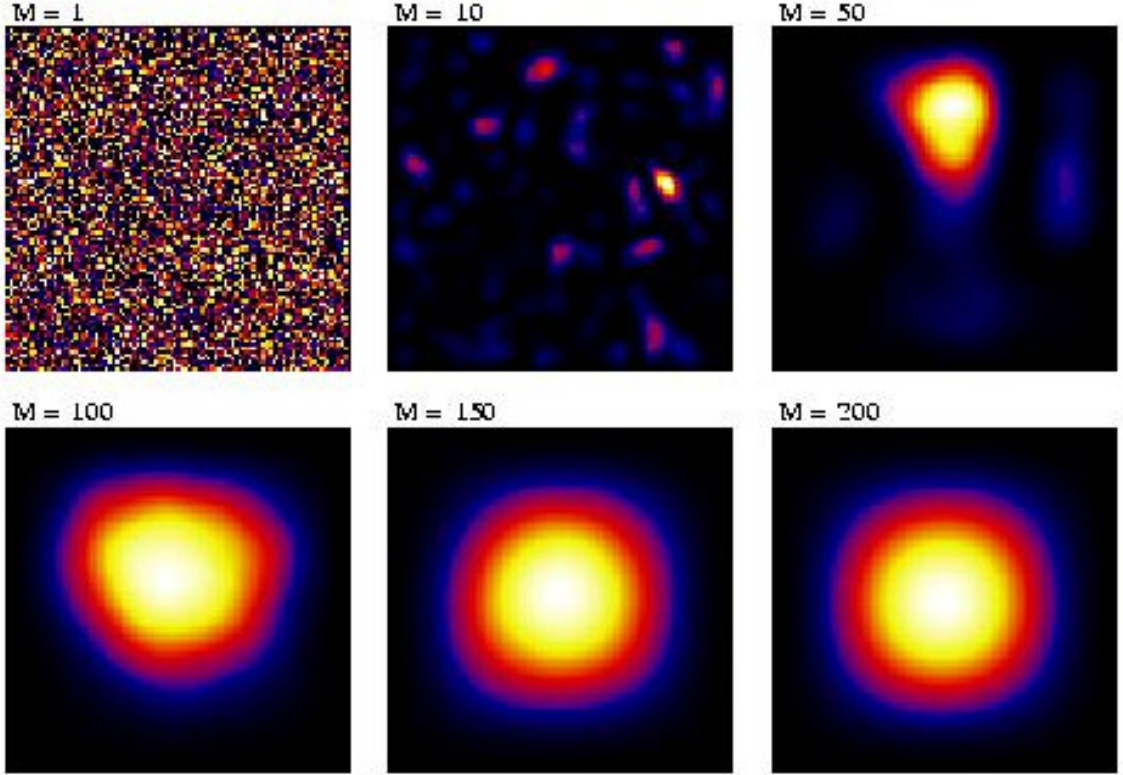

Figure 12: Intensity plots of squared wave functions obtained in Lanczos calculations with different basis sizes M for a two-dimensional hard-wall potential discretized using 200 elements ($\Delta = 0.01$). The $M = 1$ graph shows the randomly generated state that was used as the initial state in all cases. Black and white correspond to $|\Psi|^2 = 0$, and the highest $|\Psi|^2$, respectively.

Fig. 11 shows the convergence of the ground state energy in a two-dimensional calculation, with two different discretizations Δ. In accord with the above discussion, the energy converges when $M \sim L/\Delta$ in both cases. The convergence of the ground state wave function is shown in Fig. 12.

4.5 Numerical instabilities in the Lanczos method

If the Lanczos basis M is large, the procedure typically suffers from numerical instabilities. Round-off errors accumulated in the construction of the orthonormal basis states introduce some degree of non-orthogonality, which eventually leads to a complete break-down of the method. Such instabilities are often signaled by the appearance of several identical eigenvalues (recall that the Lanczos scheme should never produce degenerate states). Using double-precision arithmetic, these instabilities typically enter severely when $M \approx 500$. Stabilization methods ensuring that the basis remains orthogonal have been developed and enable much larger basis sizes, but we will not discuss these more advanced Lanczos methods here.

One can accelarate the convergence of a Lanczos calculation, thus reducing the M required and avoiding non-orthogonality problems, by starting from a state which is already close to the ground state. Such a state could be obtained using, e.g., perturbation theory, or be constructed from a Lanczos calculation with a larger Δ. Note, however, that if the initial state is a good approximation to the ground state, it may have very small overlaps with the first few excited states, and hence only the ground state is likely to be well reproduced in such a calculation.

One can target an excited states specifically by starting from a state that is orthogonal to the ground state (constructed in a prior calculation). All the Lanczos basis vectors will then have zero overlap with the ground state, and the lowest state produced will be the state with the lowest energy that does overlap with the initial state. One can in principle reproduce a large number of excited states this way, by carrying out a series of calculations in which each initial state is chosen othogonal to all the lowest states states obtained in the prior steps. In this case round-off errors can again cause problems, as they will induce some overlaps of the basis functions with the previous states. This problem can also be solved by supplementing the basis construction with a re-orthogonalization procedure.